Bloch points are sticky

Se Kwon Kim and Oleg Tchernyshyov

Department of Physics and Astronomy, Johns Hopkins University,
3400 N. Charles St., Baltimore, Maryland, 21218
(Dated: January 29, 2013)

Bloch points are magnetic topological defects resembling hedgehogs. The discrete nature of a magnetic lattice creates a periodic potential that can pin a Bloch point. The pinning force is of the order of the exchange constant, a few piconewtons in a typical ferromagnet (permalloy). A domain wall containing a Bloch point can have a sizable depinning field in the tens of oersted.

I. INTRODUCTION

Topological defects, nonlinear excitations made stable by their nontrivial topology, are ubiquitous in magnetism. They play an important role in the dynamics of magnets, mediating transitions between low-energy states. Defects come in a variety of dimensions and shapes. In a thin ferromagnetic film, where shape anisotropy keeps magnetization in the plane of the film, point-like topological defects are vortices. Away from the core, magnetization stays in the easy plane, winding clockwise or counterclockwise once as the core is encircled. At the core of a vortex, an area several nanometers across, magnetization points normal to the easy plane. The core endows the magnetization with a double twist, which is ultimately responsible for a gyrotropic force that dominates vortex dynamics.

An example of a point-like defect in three dimensions is a magnetic hedgehog, or a Bloch point,[1–6]. In the simplest case, magnetization in its vicinity has a spherically symmetric distribution,

$$\mathbf{M}(\mathbf{r}) = \pm\frac{M\mathbf{r}}{r}, \tag{1}$$

where M is magnetization length, with a typical value of 8×10^5 A/m (permalloy). More generally, a hedgehog is stable if the unit vector of magnetization $\hat{\mathbf{m}}(\mathbf{r}) \equiv \mathbf{M}(\mathbf{r})/M$ has a nonzero winding number of the second homotopy group $\pi_2(S^2)$,[7] also known as the skyrmion charge:

$$q = \frac{1}{8\pi} \int dA_i\, \epsilon_{ijk}\, \hat{\mathbf{m}} \cdot \partial_j\hat{\mathbf{m}} \times \partial_k\hat{\mathbf{m}}, \tag{2}$$

where the integral is over a closed surface surrounding the hedgehog. For a simple hedgehog (1), $q = \pm 1$.

A skyrmion number q can also be defined for a vortex on a two-dimensional surface. The skyrmion density $\epsilon_{ijk}\, \hat{\mathbf{m}} \cdot \partial_j\hat{\mathbf{m}} \times \partial_k\hat{\mathbf{m}}/8\pi$ is nonzero only if the unit vector of magnetization $\hat{\mathbf{m}}$ is non-coplanar. Therefore, the skyrmion charge of a vortex is concentrated near its core, where magnetization comes out of the easy plane. The skyrmion charge of a vortex is half-integer, $q = \pm 1/2$. This difference between a hedgehog and a vortex can be understood intuitively by noting that magnetization $\hat{\mathbf{m}}$ around a hedgehog acquires every direction on the unit sphere, whereas magnetization near a vortex core only covers half of it, e.g., the northern hemisphere. The skyrmion number of a vortex on the surface of a magnetic sample is related to its "core polarization," i.e., the direction of magnetization normal to the surface. For a vortex, a core magnetized into (out of) the surface has $q = +1/2$ ($-1/2$). For an antivortex, the relation is reversed.

Whereas magnetic vortices have been extensively studied both theoretically and experimentally and are by now well understood, isolated magnetic hedgehogs are elusive and have so far been studied mostly by theorists. (Kabanov *et al.*[8] observed Bloch points on a Bloch line, which in turn is part of a Bloch domain wall.) These objects are fascinating
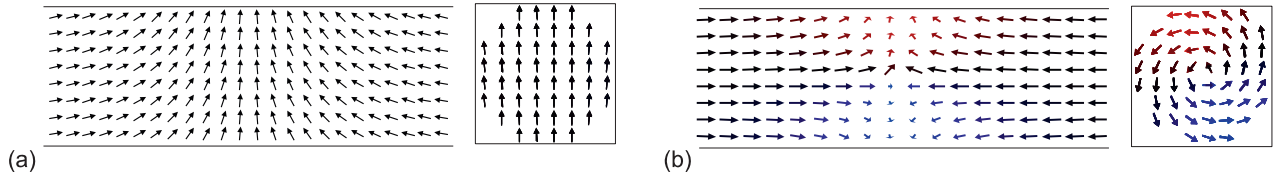

FIG. 1. (a) The transverse wall in a cylindrical nanowire of radius 10 (nm). The left (right) figure is a snapshop of magnetization at the center of the cylinder from the positive x (z) direction. The blue (red) arrows mean the positive (negative) component of magnetization along the x axis. (b) The Bloch point wall in a cylindrical nanowire of radius 30 (nm). The same color scheme as (a) is applied.

as well as important. For instance, the reversal of core magnetization in a vortex changes its skyrmion number by ± 1. One might suspect that the difference is taken by an object with unit skyrmion charge such as a Bloch point. Indeed, numerical studies have demonstrated the involvement of a Bloch point in a core reversal process.[9,10] Hedgehogs also create nontrivial magnetization dynamics. Hertel and Kirschner[11] reported an observation of "magnetic drops" behind a moving Bloch point.

Another peculiar feature of a magnetic hedgehog is the absence of a characteristic length scale. Whereas the size of a vortex core is determined by a competition between short-exchange force and shape anisotropy due to dipolar interactions, a hedgehog solution (1) is scale-invariant and thus sensitive to both short and long-wavelength physics. We may expect that the center of a hedgehog, where spatial variation of magnetization is particularly strong, can be easily pinned by lattice imperfections and even by the atomic lattice itself! In this paper we show that this is indeed the case: even the periodic potential of an atomic lattice may create a substantial landscape for a Bloch point.

We present a theoretical study of a Bloch point that is part of a domain wall in a ferromagnetic nanowire with a solid circular cross section (a solid cylinder). Thanks to shape anisotropy of dipolar interactions, such a wire has two ferromagnetic ground states with uniform magnetization along the axis of the wire. A domain wall separating two ground states can be of different types, depending on the radius R of the wire.[12–15]. For a small radius, not exceeding a few exchange lengths, a "transverse" wall is formed, Fig. 1(a). It consists of two surface defects, a vortex and an antivortex with skyrmion numbers $q = \pm 1/2$ each (negative for a head-to-head domain wall). For a larger radius, a "vortex" wall is formed, Fig. 1 (b). Contrary to its name, it contains a Bloch point, rather than a vortex, so we shall refer to it as a Bloch-point wall (BPW). The skyrmion charge of the hedgehog is ± 1 (negative for a head-to-head domain wall).

The domain-wall topology of magnetization in a magnetic wire provides an easy way to apply a force to a Bloch point: a uniform magnetic field $\mathbf{H}_0$ parallel to the axis of the wire pushes the domain wall with a force $\mu_0 Q \mathbf{H}_0$, where $Q = \pm 2\pi R^2 M$ is the magnetic charge of the domain wall (positive for a head-to-head domain wall). If the Bloch point is pinned, the wall is unable to move until the applied field is sufficiently strong to overcome the pinning force.

The pinning of a Bloch point in an atomic lattice has a simple origin. Picture a hedgehog moving through a simple cubic lattice of magnetic atoms parallel to one of the cubic axes, Fig. 2. The hedgehog's energy is lowest when it is at the center of a cubic cell ($z = 0$), farthest from the magnetic dipoles in its corners. It is highest (along that trajectory) when the hedgehog is at the center of a face ($z = a/2$). A simple model of the Bloch point's energy on this straight line is $U(z) = -U_0 \cos(2\pi z/a)$, where a is the lattice constant. The amplitude U_0 can be estimated as follows. The primary source of the pinning potential is the exchange energy $E_{\mathrm{ex}} = A \int d^3r \, \partial_i \hat{\mathbf{m}} \cdot \partial_i \hat{\mathbf{m}}$, where A is the exchange constant with the dimension of energy per unit length. We thus expect that $U_0 = cAa$, where c is a numerical constant of order 1. This gives the maximal pinning force $F_p = 2\pi c A$ that is independent of the lattice constant a. The critical field for depinning a domain wall with a Bloch point in a magnetic wire of radius R is then

$$H_c = \frac{cA}{\mu_0 M R^2} = \frac{cM}{2} \frac{\ell_{\mathrm{ex}}^2}{R^2}, \tag{3}$$

where $\ell_{\mathrm{ex}} = \sqrt{2A/\mu_0 M^2}$ is the exchange length. For a typical ferromagnet (permalloy, $A = 1.3 \times 10^{-11}$ J/m, $M = 8 \times 10^5$ A/m, $\ell_{\mathrm{ex}} = 5.7$ nm), we obtain a pinning force of order 10^{-11} N. A permalloy wire with radius $R = 50$ nm would have a sizable depinning field $H_c \approx 60$ Oe.

The paper is organized as follows. In Sec. II, we compute the lattice potential of a magnetic hedgehog and the associated critical field for a Bloch-point domain wall. In Sec. III, we compare the computed value against numerical simulations using the micromagnetic simulator OOMMF.[16] We discuss our results in Sec. IV.

II. THEORY FOR THE PINNING CRITICAL FIELD

The energy of a ferromagnet in a continuum model is given by

$$E = \int d^3r \left(A \, \partial_i \hat{\mathbf{m}} \cdot \partial_i \hat{\mathbf{m}} - \frac{\mu_0 M^2}{2} \hat{\mathbf{m}} \cdot \mathbf{h}_D - K m_z^2 \right), \tag{4}$$

where $\hat{\mathbf{m}} \equiv \mathbf{M}/M$ is the unit magnetization vector, A is the exchange constant, M is the saturation magnetization, K is an easy-axis anisotropy constant, and $\mathbf{h}_D$ is a dimensionless demagnetizing field satisfying $\nabla \cdot \mathbf{h}_D = -\nabla \cdot \hat{\mathbf{m}}$ and $\nabla \times \mathbf{h}_D = 0$. The coupling constants A, $\mu_0 M^2$, and K have dimensions of energy/length, energy/length^3, and energy/length^3, respectively. They can be used to construct an intrinsic length scale known as the exchange length, $\ell_{\mathrm{ex}} \equiv \sqrt{2A/\mu_0 M^2}$, and a dimensionless "quality factor," $Q = 2K/\mu_0 M^2$ expressing the strength of local anisotropy relative to the shape anisotropy of the demagnetizing field $\mathbf{h}_D$. Since we are interested in a weakly anisotropic system, $Q \ll 1$, we ignore the anisotropy energy for calculation of the mesh potential of BP.
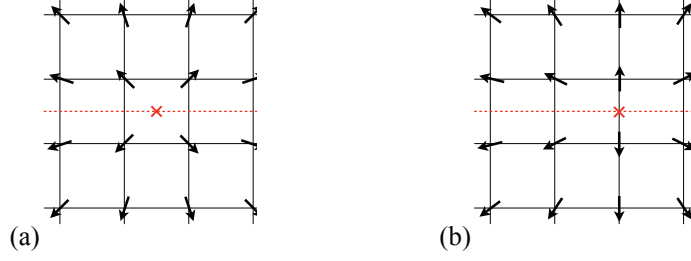
FIG. 2. Magnetization configurations with two different BP positions (cross): (a) at the center of a cubic cell and (b) at the center of a cell's face.

We have evaluated the energy of a magnetic hedgehog in a Heisenberg ferromagnet on a simple cubic lattice with nearest-neighbor exchange coupling $J = 2Aa$, which gives the same exchange energy for slow spatial variations as does the continuum version, Eq. (4). The lattice Hamiltonian is

$$E = -2Aa \sum_{\langle ij \rangle} \hat{\mathbf{m}}_i \cdot \hat{\mathbf{m}}_j + \frac{Aa^3}{4\pi\ell_{\text{ex}}^2} \sum_{i \neq j} \frac{\hat{\mathbf{m}}_i \cdot \hat{\mathbf{m}}_j - 3(\hat{\mathbf{m}}_i \cdot \hat{\mathbf{e}}_{ij})(\hat{\mathbf{m}}_j \cdot \hat{\mathbf{e}}_{ij})}{r_{ij}^3} \tag{5}$$

where $\hat{\mathbf{e}}_{ij}$ is the unit vector pointing from the site i to the site j and r_{ij} is the distance between two sites in units of the mesh size a. Spins are located at half-integer lattice points $\mathbf{r}_i = (i_1 + 1/2, i_2 + 1/2, i_3 + 1/2)$, where i_1, i_2, and i_3 are integers. We used the following Ansatz for magnetization in cylindrical coordinates $\mathbf{r} = (\rho, \phi, z)$, z being the wire axis:

$$m_\rho = \frac{s\rho \sin\phi_0}{\sqrt{s^2\rho^2 + (z - z_{\text{BP}})^2}},$$

$$m_\phi = \frac{s\rho \cos\phi_0}{\sqrt{s^2\rho^2 + (z - z_{\text{BP}})^2}} \tag{6}$$

$$m_z = \frac{z - z_{\text{BP}}}{\sqrt{s^2\rho^2 + (z - z_{\text{BP}})^2}}$$

where $(0, 0, z_{\text{BP}})$ is the location of BP, ϕ_0 is the deviation magnetization projected into the xy plane from the azimuthal direction $\hat{\phi}$, and s is a phenomenological shape factor expressing the deformation of a hedgehog inside a cylindrical wire. The shape factor was determined from numerical simulations by fitting magnetization of a static hedgehog to Ansatz (6) in the vicinity of the singularity.

Our analysis, presented in detail in Appendix A, shows that the periodic potential experienced by the hedgehog in the lattice is dominated by the first harmonic:

$$E(z_{\text{BP}}) \approx -Aa(c_{\text{ex}} - c_{\text{dip}}a^2/\ell_{\text{ex}}^2) \cos(2\pi z_{\text{BP}}/a), \tag{7}$$

where c_{ex} and c_{dip} are positive constants of order of 1 reflecting the contributions of exchange and dipolar interactions. Figure 3 shows the dependence of c_{ex} and c_{dip} on the shape factor s. In the case of the atomic lattice, $a \ll \ell_{\text{ex}}$ and the dipolar term contributes relatively little. However, in our numerical simulations the lattice constant a was comparable to the exchange length ℓ_{ex}. We therefore kept the dipolar term in Eq. (7) for comparison with the numerics.

The pinning force created by the periodic potential is

$$F_p(z_{\text{BP}}) = -E'(z_{\text{BP}}) \approx 2\pi A(c_{\text{ex}} - c_{\text{dip}}a^2/\ell_{\text{ex}}^2) \sin(2\pi z_{\text{BP}}/a). \tag{8}$$

It matches the external force of the applied field, $F_Z = \mu_0 QH$, where $Q = 2\pi MR^2$ is the wall's magnetic charge, until F_p reaches its maximum value at $z_{\text{BP}} = a/4$. This gives a critical field for depinning,

$$H_c = (c_{\text{ex}} - c_{\text{dip}}a^2/\ell_{\text{ex}}^2)\frac{M}{2}\frac{l_{ex}^2}{R^2}. \tag{9}$$

III. NUMERICAL SIMULATION

We performed numerical simulation with the micromagnetic package OOMMF[16] to verify our calculation of critical fields. The simulated sample has the following material parameters: exchange constant $A = 1.0 \times 10^{-11}$ J/m,
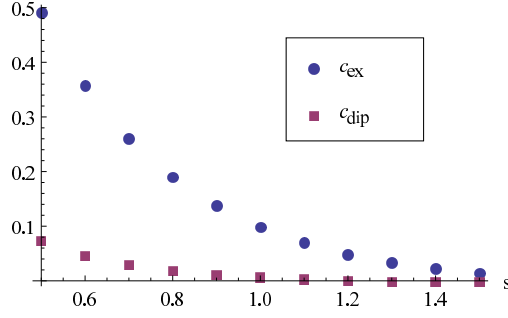
FIG. 3. Dependence of c_{ex} and c_{dip} on the shape factor s.
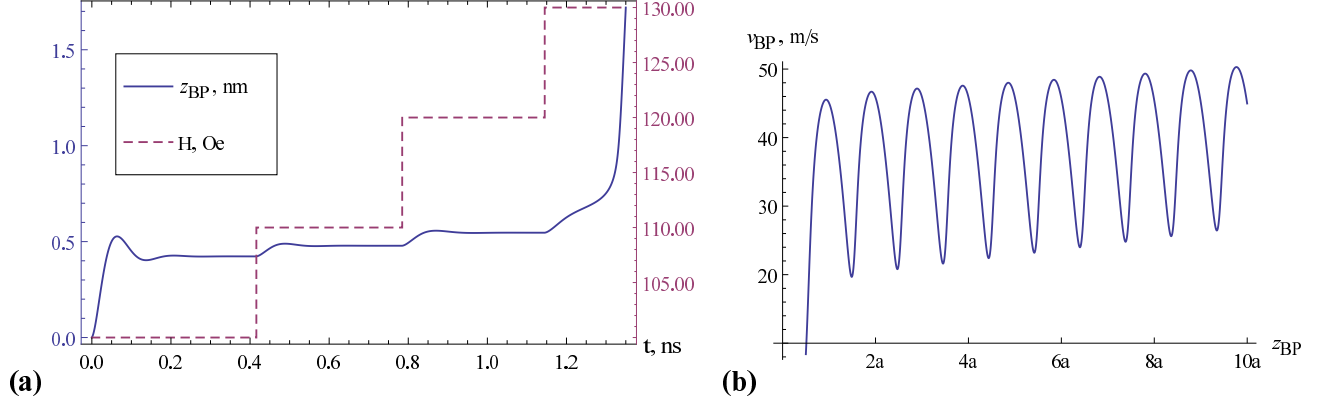

(a)

(b)

FIG. 4. (a) The position of the Bloch point and external field as a function of time (b) The velocity of the Bloch point as a function of its position

saturation magnetization $M = 10^6$ (A/m), easy-axis anisotropy $K = 10^4$ J/m^3, gyromagnetic ratio $\gamma_0 = 2.21 \times 10^5$ m/(A s), and a damping constant $\alpha = 0.3$. (We used a large damping constant to reduce simulation time.) The exchange length for this material is $\ell_{ex} = 4.0$ nm and the quality factor is $Q = 0.016$. A small easy axis anisotropy helps stabilize a domain wall with a Bloch point.[12] Since $Q \ll 1$, we did not include the anisotropy energy in the calculation of the mesh potential. We used two different sample geometries: (i) radius $R = 10$ nm and length $L = 200$ nm; (ii) radius $R = 15$ nm and length $L = 300$ nm. To determine the critical field, we applied the external field increasingly starting at 100 Oe and 30 Oe and increasing it in steps of 10 Oe and 5 Oe for the narrow and wide wires, respectively. Figure 4 shows the position of the Bloch point z_{BP} as a function of time for the narrow wire with a lattice constant $a = 1.7$ nm.

The results are summarized in Fig. 5. It can be seen that the depinning field H_c does not extrapolate to zero as the size of a unit cell a in the simulation is reduced. This behavior of a Bloch-point domain wall is strikingly different from the typical behavior of domain walls in numerical simulations. Ordinarily, the effects of lattice discretization
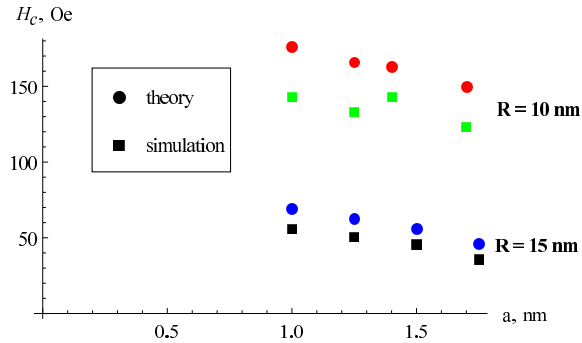

FIG. 5. Theoretical and simulated critical fields

become unnoticeable when the mesh size is reduced below half the exchange length ℓ_{ex}. The finest mesh size in our simulations, $a = 1$ nm, is much smaller than $\ell_{\text{ex}} = 4.0$ nm, yet the lattice effects do not subside. Furthermore, the critical field *increases* as the mesh size decreases. The main reason for this effect comes from the dependence of the shape factor on the mesh size. As the mesh size decreases, the shape factor decreases, which results in increase in c_{ex} (see the figure 3). Magnetization around BP becomes more isotropic as the mesh size decreases.

The mesh potential also affects dynamics of a BPW under the external field above the critical field. The velocity of BPW oscillates and this oscillation is periodic in the position of BPW, which means that the mesh potential for BP is responsible for the oscillation. See (b) in the figure 4 for an example. The slight increase of the average velocity as a function of time can be attributed to the attractive force between the volume magnetic charge of BPW and the surface magnetic charge at the end of the cylinder.

IV. DISCUSSION

Topological defects in magnets can be pinned by a periodic potential of the underlying magnetic lattice. When lattice discretization is employed to simulate a continuous magnetic medium, this periodic potential is an artifact that can be removed by choosing a sufficiently fine mesh. For a domain wall, the lattice period should be small compared to the wall width; for a vortex, smaller than its core. A magnetic hedgehog turns out to be exceptional in this regard because it has no characteristic length scale. As a result of that, the amplitude of the periodic pinning potential of the lattice is linearly proportional to the lattice constant. Thus the maximal pinning force is independent of the lattice constant and is of the order of the exchange constant, $A = 1.3 \times 10^{-11}$ N in permalloy.

In this paper we have estimated the strength of the periodic pinning potential experienced by a magnetic hedgehog in a simple cubic lattice. The estimate is in good agreement with micromagnetic simulations, which yield a finite pinning field for a domain wall containing a Bloch point, even when the unit cell is much smaller than the exchange length. We expect that Bloch points are strongly pinned by the atomic lattice in ferromagnets. The strength of pinning should be reduced by thermal and quantum fluctuations, which can create a core where magnetization vanishes. Numerical estimates[6,17] show that the core size induced by thermal fluctuations is small, comparable to the lattice spacing at room temperature.

Appendix A: Mesh potential calculation

The exchange and dipolar energies of a ferromagnet (5) in the presence of a Bloch point at $(0, 0, z_{\text{BP}})$ are

$$E_{\text{ex}}(z_{\text{BP}}) = -2Aa \sum_{\langle ij \rangle} \hat{\mathbf{m}}_i \cdot \hat{\mathbf{m}}_j$$

$$E_{\text{dip}}(z_{\text{BP}}) = \frac{Aa^3}{4\pi\ell_{\text{ex}}^2} \sum_{i \neq j} \frac{\hat{\mathbf{m}}_i \cdot \hat{\mathbf{m}}_j - 3(\hat{\mathbf{m}}_i \cdot \hat{\mathbf{e}}_{ij})(\hat{\mathbf{e}}_{ij} \cdot \hat{\mathbf{m}}_j)}{|\mathbf{r}_i - \mathbf{r}_j|^3}, \tag{A1}$$

with $\hat{\mathbf{m}}_i$ given by Ansatz (6). Being periodic functions of z_{BP} with a lattice period a, these expressions can be written as Fourier series:

$$E_{\text{ex}}(z_{\text{BP}}) - E_{\text{ex}}(0) = -Aa \sum_{n=1}^{\infty} c_{\text{ex},n} \cos(2\pi n z_{\text{BP}}),$$

$$E_{\text{dip}}(z_{\text{BP}}) - E_{\text{dip}}(0) = \frac{Aa^3}{\ell_{\text{ex}}^2} \sum_{n=1}^{\infty} c_{\text{dip},n} \cos(2\pi n z_{\text{BP}}). \tag{A2}$$

The subtraction of the $z_{\text{BP}} = 0$ term improves convergence of the energy in a finite lattice. The Fourier amplitudes $c_{\text{ex},n}$ and $c_{\text{dip},n}$ depend on the shape factor s; $c_{\text{dip,n}}$ also depends on the angle ϕ_0. Overall signs of formula is determined so that the first harmonics $c_{\text{ex},1}$ and $c_{\text{dip},1}$ are positive. The shape factor s and the angle ϕ_0 were obtained by fitting magnetization of an OOMMF solution at the eight mesh points closest to a Bloch point at $z_{\text{BP}} = 0$.

The Fourier amplitudes $c_{\mathrm{ex,n}}$ can be computed analytically by applying Poisson's formula to the index i_3 along the z-axis,

$$\sum_{i_3=-\infty}^{\infty} f(z+i_3) = \sum_{n=-\infty}^{\infty} e^{-2\pi i n z} \int dz' e^{2\pi i n z'} f(z').$$

We thus obtain

$$c_{\mathrm{ex},n} = 2 \sum_{i_1,i_2=-\infty}^{\infty} \int dz \cos(2\pi n z)$$
$$\times \left[4(-1)^n \left(\frac{s\mathbf{x}_i + z\hat{\mathbf{z}}}{|s\mathbf{x}_i + z\hat{\mathbf{z}}|} \cdot \frac{s\mathbf{x}_i - s\hat{\mathbf{x}} + z\hat{\mathbf{z}}}{|s\mathbf{x}_i - s\hat{\mathbf{x}} + z\hat{\mathbf{z}}|} - 1 \right) + 2 \left(\frac{s\mathbf{x}_i + (z+1/2)\hat{\mathbf{z}}}{|s\mathbf{x}_i + (z+1/2)\hat{\mathbf{z}}|} \cdot \frac{s\mathbf{x}_i + (z-1/2)\hat{\mathbf{z}}}{|s\mathbf{x}_i + (z-1/2)\hat{\mathbf{z}}|} - 1 \right) \right]. \quad (A3)$$

Here $\mathbf{x}_i = (i_1 + 1/2, i_2 + 1/2, 0)$ is the projection of $\mathbf{r}_i$ onto the xy plane and $\phi_0 = \pi/2$ is used. This expression is dominated by the $n = 1$ term. In practice it suffices to use only $n = 1$ and $i_1, i_2 = -1, 0, 1$. c_{ex} used in the main part of the paper is $c_{\mathrm{ex},1}$ calculated with $i_1, i_2 = -1, 0, 1$.

The Fourier amplitudes $c_{\mathrm{ex},1}$ and $c_{\mathrm{dip},1}$ have also been evaluated numerically. After setting the maximum value on $I \equiv \max(|i_1|, |i_2|, |i_3|)$ in Eq.(A1), we computed the dependence of E_{ex} and E_{dip} on z_{BP} by increasing z_{BP} from 0 to 1 in steps of 0.1. We then extracted $c_{\mathrm{ex},1}$ and $c_{\mathrm{dip},1}$ by a Fourier transformation. These coefficients converge rapidly as I increases and $I = 10$ provides good accuracy. c_{dip} used in the main part of the paper is numerically calculated $c_{\mathrm{dip},1}$.

[1] E. Feldtkeller, Z. Angew. Phys. **19**, 530 (1965).
[2] W. Döring, J. Appl. Phys. **39**, 1006 (1968).
[3] K. Y. Guslienko, W. Scholz, R. W. Chantrell, and V. Novosad, Phys. Rev. B **71**, 144407 (2005).
[4] K. Y. Guslienko, X. F. Han, D. J. Keavney, R. Divan, and S. D. Bader, Phys. Rev. Lett. **96**, 067205 (2006).
[5] O. Pylypovskyi, D. Sheka, and Y. Gaididei, Phys. Rev. B **85**, 224401 (2012).
[6] K. Lebecki, D. Hinzke, U. Nowak, and O. Chubykalo-Fesenko, Phys. Rev. B **86**, 094409 (2012).
[7] G. E. Volovik, J. Phys.: Condens. Matter **20**, L83 (1987).
[8] Y. P. Kabanov, L. M. Dedukh, and V. I. Nikitenko, JETP Lett. **49**, 637 (1989), [Pis'ma Zh. Eksp. Teor. Fiz. **49**, 551 (1989)].
[9] A. Thiaville, J. García, R. Dittrich, J. Miltat, and T. Schrefl, Phys. Rev. B **67**, 094410 (2003).
[10] R. Hertel and C. M. Schneider, Phys. Rev. Lett. **97**, 177202 (2006).
[11] R. Hertel and J. Kirschner, J. Mag. Magn. Mater. **278**, L291 (2004).
[12] R. Wieser, U. Nowak, and K. Usadel, Phys. Rev. B **69**, 064401 (2004).
[13] R. Wieser, E. Vedmedenko, P. Weinberger, and R. Wiesendanger, Phys. Rev. B **82**, 144430 (2010).
[14] N. A. Usov, A. Zhukov, and J. Gonzalez, J. Mag. Magn. Mater. **316**, 255 (2007).
[15] M. Yan, A. Kákay, S. Gliga, and R. Hertel, Phys. Rev. Lett. **104**, 057201 (2010).
[16] M. J. Donahue and D. G. Porter, National Institute of Standards and Technology Report No. NISTIR 6376, http://math.nist.gov/oommf (1999).
[17] R. G. Elías and A. Verga, Eur. Phys. J. B **82**, 159 (2011).